Molecular Biology of the Cell
Vol. 8, 2089–2099, October 1997

Transport of Myosin II to the Equatorial Region without Its Own Motor Activity in Mitotic *Dictyostelium* Cells

Shigehiko Yumura*† and Taro Q.P. Uyeda‡

*Department of Biology, Faculty of Science, Yamaguchi University, Yamaguchi 753, and ‡Bionic Design Group, National Institute for Advanced Interdisciplinary Research, and Mechanical Engineering Laboratory, AIST, Tsukuba, Ibaraki 305, Japan

Submitted April 29, 1997; Accepted July 24, 1997
Monitoring Editor: David Drubin

Fluorescently labeled myosin moved and accumulated circumferentially in the equatorial region of dividing *Dictyostelium* cells within a time course of 4 min, followed by contraction of the contractile ring. To investigate the mechanism of this transport process, we have expressed three mutant myosins that cannot hydrolyze ATP in myosin null cells. Immunofluorescence staining showed that these mutant myosins were also correctly transported to the equatorial region, although no contraction followed. The rates of transport, measured using green fluorescent protein-fused myosins, were indistinguishable between wild-type and mutant myosins. These observations demonstrate that myosin is passively transported toward the equatorial region and incorporated into the forming contractile ring without its own motor activity.

INTRODUCTION

Cytokinesis of animal and lower eukaryotic amoeba cells is driven by constriction of the contractile ring. The contractile ring contains circumferential filaments of conventional myosin, or simply myosin hereafter, and actin filaments (reviewed by Mabuchi, 1986). There is cytological (Mabuchi and Okuno, 1977) and molecular genetic (De Lozanne and Spudich, 1987; Knecht and Loomis, 1987) evidence that myosin provides force for constriction of the contractile ring.

The contractile ring is a highly transient structure and its assembly and disassembly are precisely regulated both spatially and temporally. Classic cytological studies using dividing eggs have established that the mitotic spindle ultimately determines the position of the contractile ring (reviewed by Mabuchi, 1986; Rappaport, 1991; Strome, 1993). Despite extensive research, the nature of the signal from the spindle to the cortex is still elusive. The molecular mechanism of accumulating myosin and other components of the contractile ring to the equatorial region is also still unknown.

Recently, the cellular slime mold *Dictyostelium discoideum* has emerged as an excellent model experimental system to study cytokinesis with molecular and cell biological approaches. For instance, *Dictyostelium* provided the opportunity to prove genetically the critical roles myosin plays in cytokinesis, by inactivating the single-copy myosin heavy chain gene (*mhc*A) either by homologous recombination (De Lozanne and Spudich, 1987) or by antisense silencing (Knecht and Loomis, 1987). These studies also showed that the cells unable to carry out cytokinesis become large and multinucleated and eventually lyse in suspension culture but on a solid substratum can tear themselves into smaller pieces by amoeboid movement and grow. The latter behavior, named "traction-mediated cytofission," makes it possible to express mutated forms of myosin in *mhc*A$^-$ cells. Furthermore, a chimeric gene that consists of *mhc*A fused to the green fluorescent protein (GFP) gene was expressed in *mhc*A$^-$ *Dictyostelium* cells and was found to be functional in vivo (Moores *et al.*, 1996). This new technique, as well as the more classic method of introducing fluorescently labeled myosin into live cells (Chu and Fukui, 1996; Yumura, 1996), enabled real time tracing of myosin localization in vivo. Thus, a wide spectrum of tools is

† Corresponding author.

now available to test a particular hypothesis concerning myosin's role or its regulation during cytokinesis in *Dictyostelium*.

In the popular "cortical flow model," the cortical components are actively transported to the equatorial region to assemble the contractile ring. In this model, tension is generated more or less uniformly in the metaphase cortex, but subsequent polar relaxation or equatorial stimulation triggers the cortex in each half of the cell to pull itself toward the equatorial region and align circumferentially in the plane of division (Bray and White, 1988). It is assumed that this transport process is driven by active cortical tension. Because cortical tension is generated by active interactions between cortical actin and myosin filaments (Reines and Clarke, 1985; Pasternak *et al.*, 1989; Kuczmarski *et al.*, 1991; Yumura, 1991), it is further assumed that the transport process is ultimately powered by the motor activity of myosin (DeBiasio *et al.*, 1996).

We have tested this point by analyzing the behavior of enzymatically inactive mutant *Dictyostelium* myosins recently isolated by Ruppel and Spudich (1996). Our results demonstrate the independence of the motor activity of myosin for its movement to the equatorial region. Possible mechanisms of myosin accumulation toward the equatorial region are discussed.

EXPERIMENTAL PROCEDURES

Construction of Mutant Myosin Genes

Standard methods were used for all DNA manipulations (Ausubel *et al.*, 1994).

The expression vector for GFP-myosin was constructed based on pBIG-GFPmyo (Moores *et al.*, 1996), a kind gift from S. Moores and J. Spudich (Stanford University). Briefly, pBIG-GFPmyo carries extrachromosomal replication sequences in *Dictyostelium*, the neomycin-resistance gene, and the GFP gene fused to the actin 15 promoter and to the wild-type *mhc*A gene. pBIG-GFPmyo was first modified to include the S65T mutation in the GFP gene, which has enhanced fluorescence properties (Heim *et al.*, 1995; the S65T GFP gene was a kind gift from Dr. R. Tsien [University of California at San Diego, La Jolla]). Additionally, to facilitate future subcloning process, the vector backbone was exchanged from pBIG to pTIKL (Liu, Ito, Lee, and Uyeda, personal communication), a derivative of pBIG, which lacks *Nco*I and *Kpn*I sites. The resultant plasmid pTIKLGFPS65Tmyo was used to express the fluorescent wild-type myosin.

The three mutant *mhc*A genes carrying E476K, E459V and F481C/N483K mutations were generous gifts from K. Ruppel and J. Spudich. They were supplied on pBIG in the form of fusion with the actin 15 promoter and were used without modification to express the nonfluorescent form for immunofluorescence staining. To engineer the GFP-fused E476K, the *Eco*NI–*Nco*I fragment of pBIGE476K was used to replace the corresponding sequence in pTIKLGFPS65Tmyo.

Overexpression of soluble head fragments was achieved as follows. The plasmid DH12.1R (Anson *et al.*, 1996; a generous gift from Dr. D. Manstein [Max-Planck Institute, Dortmund, Germany]) drives overexpression of M761–1R, a wild-type myosin head fragment truncated at amino acid residue 761 and fused to one unit of triple α-coiled coil repeat of the α-actinin gene, followed by the histidine tag. The E476K mutation was introduced into DH12.1R using the *Eco*NI–*Bgl*II sites.

The pBIG- or pTIKL-based plasmids carrying each mutation were used to transfect HS1, an *mhc*A$^-$ *Dictyostelium* cell line (Ruppel *et al.*, 1994). Transformation was carried out by electroporation as described previously (Egelhoff *et al.*, 1991b). DH12.1R and its derivative were coelectroporated into HS1 cells together with a plasmid that carried the Ddp2 open reading frame that is required *in trans* for extrachromosomal replication of DH12.1R (Manstein and Hunt, 1995).

Culture of Dictyostelium Cells

Wild-type Ax2 and HS1 cells were maintained on 9-cm plastic plates containing HL5 (Sussman, 1987) supplemented with 60 μg/ml penicillin and 60 μg/ml streptomycin (PS). HS1 cells carrying one of the G418-resistance plasmids were grown on plates containing HL5, PS, and 12 μg/ml G418. For cell biological experiments, cells were harvested from these plates and washed with BSS (10 mM NaCl, 10 mM KCl, and 3 mM $CaCl_2$).

For the purification of mutant myosins, cells were grown on 20 × 20 cm^2 square plastic plates containing 100 ml of HL5, PS, and 12 μg/ml G418 at 21°C. When the culture had reached confluence, medium was changed to a fresh 200 ml of HL5 and PS, without G418, and the plates were incubated for additional 24–36 h on a rotary shaker.

Both G418-sensitive and -resistant cells were preincubated in 9-cm plates containing HL and PS for 24 h at 21°C before the cell division assay. They were then detached from the plates using 10-ml pipettes, counted, and inoculated in 200-ml flasks containing 50 ml of HL5 and PS at a density of around 2×10^5 cells/ml. The flasks were shaken at 200 rpm on a rotary shaker at 21°C, and the cell density was monitored at 12-h intervals until the wild-type cells have reached the stationary phase.

Introduction of Labeled Protein

Wild-type myosin was purified from *Dictyostelium* cells (Ax2) and labeled with 5-iodoacetoamide fluorescein (IAF) as described previously (Yumura, 1996). Bovine serum albumin (BSA) was labeled with tetramethylrhodamine (Yumura *et al.*, 1995). These proteins were introduced into cells by electroporation as described previously (Yumura *et al.*, 1995).

Fluorescence Microscopy

Cells were washed by centrifugation and suspended in BSS. They were settled on a coverslip for 10 min and overlaid with a thin sheet of agar as described previously (Yumura, 1996). The coverslip was fixed on an aluminum folder with a 1-cm^2 square hole for observation. The samples were observed by an inverted fluorescence microscope (TMD300, Nikon, Tokyo, Japan) equipped with a silicone intensified camera (C2400–08, Hamamatsu Photonics, Bridgewater, NJ). Fluorescence of GFP was observed by using the B2 fluorescence cassette (Nikon, B-2A) and of rhodamine was done by using the G fluorescence cassette (Nikon, G-2A). The fluorescence images were digitized to 8 bits (256 gray scale) by an Argus 50 video processor (Hamamatsu Photonics, Hamamatsu, Japan) and recorded on VHS video tapes. Eight frames of sequential images were averaged real time. They were obtained sequentially for eight 30-s periods with 10- to 30-s intervals to minimize damage to the cells by illumination. The acquisition conditions were set so that the highest brightness did not exceed the saturation level. To estimate the rate of myosin's movement to the equator, the fluorescence intensity of several fixed areas of 10 × 10 pixels along the spindle axis was quantified. The linearity within the 256 gray levels in this assay was confirmed using fluorescein isothiocyanate-labeled BSA previously (Yumura *et al.*, 1995). The ratio images between IAF and rhodamine images were calculated by the NIH Image software (Yumura, 1996).

Immunofluorescence microscopy was done by the agar-overlay method according to Yumura *et al.* (1984).

Preparation of Proteins

Typically, 10–15 g of cells were obtained from six plates (20 × 20 cm^2) for each preparation. Wild-type M761–1R was purified according to the procedure of Manstein and Hunt (1995) with several modifications. Briefly, cells were washed twice in 5 mM NaN_3 in 10 mM Tris-HCl, pH 7.4, and resuspended in lysis buffer [25 mM HEPES, pH 8.0, 5 mM EDTA, 7 mM β-mercaptoethanol (βME), and a mixture of proteinase inhibitors (Manstein and Hunt, 1995)] at 5 vol/g of cells. The suspension was mixed with lysis buffer containing 1% Triton X-100 at 4 vol/g, incubated on ice for 10 min, and centrifuged at 36,000 × *g* for 30 min. The pellets were resuspended in the wash buffer (10 mM HEPES, pH 7.4, 1 mM EDTA, and 7 mM βME) and centrifuged at 36,000 × *g* for 15 min. The washed pellets were extracted with extraction buffer (10 mM HEPES, pH 7.4, 50 mM NaCl, 5 mM $MgCl_2$, 4 mM ATP, and 7 mM βME) at 2 vol/g of cells and centrifuged at 250,000 × *g* for 1 h. The supernatant was loaded onto a column containing 1 ml of Ni-nitrilotriacetic acid agarose resin (Qiagen, Hilden, Germany). The column was extensively washed with the HS/ATP buffer (10 mM HEPES, pH 7.4, 200 mM NaCl, 5 mM $MgCl_2$, 1 mM ATP, and 7 mM βME), followed by the second extensive wash with a solution containing 40 mM imidazole, pH 7.4, and 7 mM βME. The protein was eluted with 5 ml of 150 mM imidazole and 7 mM βME and, after addition of EDTA to 1 mM, was dialyzed against a buffer containing 25 mM HEPES, pH 7.4, 25 mM KCl, 0.1 mM EDTA, and 1 mM dithiothreitol (DTT).

The mutant E476K/M761–1R was unable to be purified as above, because it hardly sedimented with the crude cytoskeleton fraction even in the absence of exogenous ATP. Thus, it was purified from the supernatant fraction as follows. The cells were washed twice in 10 mM Tris, pH 7.4, and resuspended in lysis buffer (25 mM HEPES, pH 7.4, 50 mM NaCl, 5 mM $MgCl_2$, 4 mM ATP, 7 mM βME, and a mixture of proteinase inhibitors) at 5 vol/g of cells. The suspension was mixed with lysis buffer containing 1% Triton X-100 (4 vol/g) and immediately centrifuged at 36,000 × *g* for 30 min. The supernatant was loaded onto a Q-Sepharose (Pharmacia Biotech, Tokyo, Japan) column preequilibriated with buffer Q (10 mM HEPES, pH 7.4, 50 mM NaCl, 1 mM $MgCl_2$, 0.1 mM ATP, and 7 mM βME), and the bound proteins were eluted with a linear gradient of NaCl from 50 to 300 mM in buffer Q. Fractions containing E476K/M761–1R were identified by dot blotting using an anti-histidine tag monoclonal antibody (Dianova, Hamburg, Germany), pooled, and loaded onto a 1 ml of Ni-NTA agarose column. The column was washed and eluted as described above, and the eluted protein was dialyzed against a buffer containing 25 mM HEPES, pH 7.4, 25 mM KCl, 0.1 mM EDTA, and 1 mM DTT.

Rabbit skeletal muscle actin was prepared by the method of Spudich and Watt (1971). The concentrations of these proteins were determined spectrophotometrically with extinction coefficients of 0.62 cm^2/mg at 290 nm for actin (Gordon *et al.*, 1976) and 0.80 cm^2/mg at 280 nm for M761–1R (Manstein, personal communication).

ATPase Assays

Steady-state ATPase activities were determined by measuring release of phosphate at 30°C by the method of Kodama *et al.* (1986) under the conditions described by Ruppel *et al.* (1994). The reaction mixtures for the assay of MgATPase activity contained 25 mM imidazole, pH 7.5, 25 mM KCl, 4 mM $MgCl_2$, 1 mM DTT, and 1 mM ATP, with or without filamentous actin. The reaction mixture for high salt CaATPase activity measurements was 0.6 M KCl, 5 mM $CaCl_2$, 1 mM ATP, 1 mM DTT, and 10 mM imidazole, pH 7.5.

Western Blotting

Total cell lysates were separated by SDS-PAGE (7.5% polyacrylamide), blotted onto a nitrocellulose membrane, and probed with anti-*Dictyostelium* myosin heavy chain antibodies as described previously (Uyeda and Spudich, 1993).

RESULTS

Time Course of Myosin Behavior during Cytokinesis

Myosin was isolated from *Dictyostelium* cells and labeled with IAF. Labeled myosin had actin-activated ATPase activities comparable to unlabeled myosin and could assemble into filaments in vitro, as described previously (Yumura, 1996). The labeled myosin was introduced into wild-type Ax2 cells by electroporation and the IAF fluorescence was followed within single cells from prometaphase through cytokinesis (Figure 1). The stage of cell cycle was judged from the observation of nuclei by phase-contrast microscopy (Kitanishi-Yumura and Fukui, 1989). Some myosin was distributed in the cortical region and diffusely in the prometaphase endoplasm (Figure 1b). The endoplasmic myosin decreased and accumulated fairly uniformly in the cortical region during metaphase (Figure 1c). The increase of cortical myosin may underlie the increase of global cortical tension in prometaphase, when *Dictyostelium* cells round up (Kitanishi-Yumura and Fukui, 1989), similarly to dividing animal cells. The transport of cortical myosin toward the equatorial region along the cortex started at the onset of anaphase when the long axis of the cell increased as two daughter nuclei separated. Within 4.0 ± 0.5 min (mean ± SD, n = 7), accumulation of cortical myosin to the equatorial region was completed. The average velocity of myosin transport was calculated to be about 2.9 μm/min from the time-dependent changes of the fluorescence intensity at several fixed areas along the spindle axis.

To examine whether the apparent concentration of myosin in the equatorial region was affected by the exclusion volume of intracellular organelles, IAF-labeled myosin and tetramethylrhodamine-labeled BSA was simultaneously introduced into cells (Figure 2). A ratio image between the two fluorescence intensities confirmed that myosin is indeed highly concentrated in the equatorial region. Filamentous structures of myosin were sometimes observed along the contractile ring (Figure 1k) but in many cases were not clearly resolved through a video camera.

Furrowing and constriction of this region followed and cell division was completed to yield two daughter cells. The constriction took 15.9 ± 3.5 min (mean ± SD, n = 13) after the onset of telophase. The intensity of fluorescence due to localized myosin did not diminish after division and persisted in the tail region of newly formed daughter cells, which migrated away from each other.

Nonhydrolyzer Myosin Is Also Transported to the Equatorial Region

We were interested to know whether this active process of myosin transport is dependent on the motor

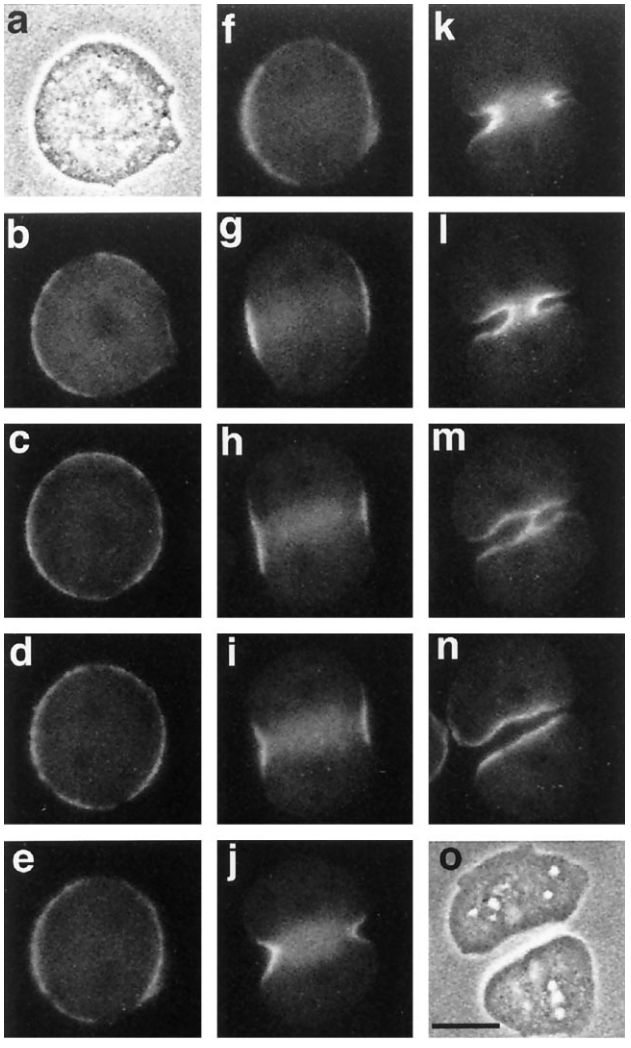

Figure 1. Dynamic distribution of fluorescently labeled myosin during mitosis in a living *Dictyostelium* cell. Fluorescence images (b–n) and phase-contrast images (a and o) were sequentially taken from a single cell (a, 0 s; b, 5 s; c, 2 min and 10 s; d, 4 min and 46 s; e, 5 min and 18 s; f, 5 min and 49 s; g, 8 min and 28 s; h, 10 min and 3 s; i, 10 min and 35 s; j, 13 min and 46 s; k, 15 min and 52 s; l, 19 min and 35 s; m, 23 min and 48 s; n, 25 min and 23 s; o, 28 min and 15 s. The cell in a is in prometaphase as judged by the loss of nucleolus. Myosin was concentrated in the cortical region at metaphase and then moved toward the equatorial region during anaphase. Contraction of the contractile ring followed and two daughter cells were produced at 15.9 ± 3.5 min (n = 13) after the onset of constriction of the furrow. Filamentous structures of myosin were sometimes observed along the contractile ring but were not adequately resolved in this particular sequence. Bar, 10 μm.

activity of myosin itself. This point can be examined experimentally by observing behavior of mutant myosins with no motor activity. In this study we used the nonhydrolyzer class mutants, which have no detectable ATPase activity and motor activity in vitro due to the inability to break the phosphodiester bond between β and γ phosphates of ATP (Ruppel and Spudich, 1996).

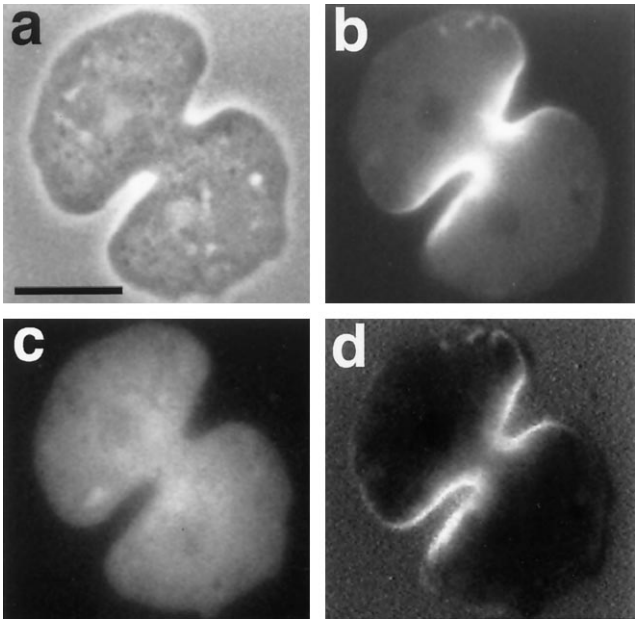

Figure 2. Distribution of IAF-labeled myosin and rhodamine-labeled BSA in the same cell. Phase-contrast micrograph (a) and fluorescence micrographs showing distribution of IAF-labeled myosin (b) and rhodamine-labeled BSA (c). (d) Ratio of intensities of fluorescence from IAF and rhodamine. Bar, 10 μm.

Each of the three nonhydrolyzer class mutant *mhc*A genes, *E476K*, *E459V*, and *F481C/N483K* (a double mutant), was individually transformed into *mhc*A$^-$ *Dictyostelium* cells (Ruppel *et al.*, 1994). Expression level of each mutant myosin in these cells was comparable with that of wild-type myosin expressed in *mhc*A$^-$ cells or with that of the endogenous myosin in wild-type cells (Figure 3). Ruppel and Spudich (1996) reported that *mhc*A$^-$ cells expressing each of these mutant myosins cannot divide in suspension culture or form fruiting bodies, but these authors did not show the actual data. We, therefore, repeated the cell division assay (Figure 4). *mhc*A$^-$ cells expressing each one of the mutant myosins did not multiply in number over a period of 4 d and became very large and multinucleated, similarly to the parental *mhc*A$^-$ cells. This result confirms the previous report (Ruppel and Spudich, 1996) that these mutant myosins are not functional in vivo.

We then examined whether these mutant myosins are accumulated in the equatorial region of cells in telophase, as judged by the presence of two small and condensed nuclei (for typical telophase nuclei, see Kitanishi-Yumura and Fukui, 1989). Immunofluorescence studies showed that all three nonhydrolyzer myosins were concentrated in the equatorial region (Figure 5). Myosin molecules existed predominantly

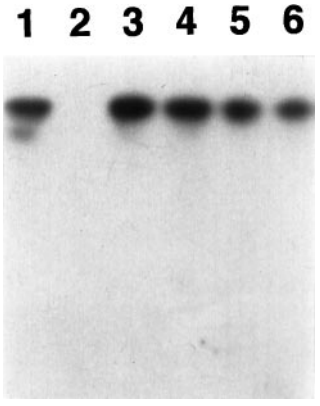

Figure 3. Western blot analysis of whole cell lysates. Whole cell lysates prepared from 0.5 μg of cells were loaded in each lane and probed with antibodies against myosin heavy chain. Lane 1, wild-type Ax2 cells; lane 2, *mhc*A$^-$ cells; lane 3, *mhc*A$^-$ cells expressing recombinant wild-type myosin; lane 4, *mhc*A$^-$ cells expressing E459V myosin; lane 5, *mhc*A$^-$ cells expressing E476K myosin; lane 6, *mhc*A$^-$ cells expressing F481C/N483K myosin.

in the filamentous form, mostly parallel to the plane of equator. The fact that all three independent mutant nonhydrolyzer myosins showed the same localization indicates that this localization is a general phenotype for the nonhydrolyzer class mutant myosins (Figure 5, b–d).

*mhc*A$^-$ cells expressing each of the mutant myosin were able to grow and divide on solid substratum without agar overlay. By an analogy to the behavior of well-characterized parental *mhc*A$^-$ cells, we speculate that the division events of these cells in the absence of the agar overlay are mostly through a process called "attachment-assisted mitotic cleavage," recently reported by Neujahr *et al.* (1997). However, these "pseudocontractile rings" of *mhc*A$^-$ cells expressing one of the nonhydrolyzer myosins showed little, if any, sign of constriction under the conditions of agar overlay. Cells expressing wild-type myosin were able to complete cytokinetic cleavage even under the agar overlay (Figure 1).

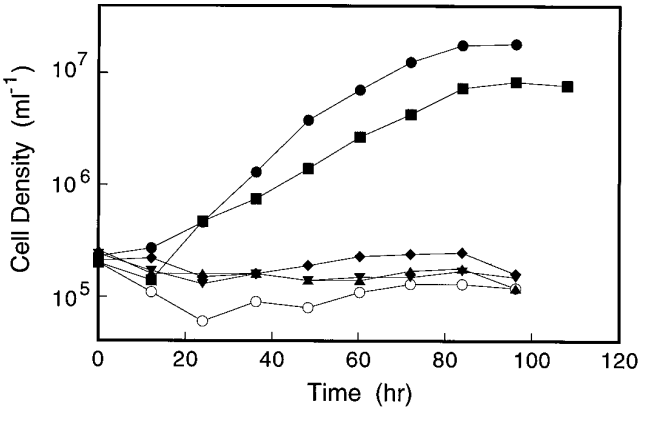

Figure 4. Suspension growth of wild-type and mutant cells. Cells were inoculated into flasks containing the HL5 medium at a density of around 2×10^5 cells/ml at time 0 and vigorously shaken on a rotary shaker at 21°C. The cell densities were monitored every 12 h. ●, Wild-type cells; ○, *mhc*A$^-$ cells; ■, *mhc*A$^-$ cells expressing recombinant wild-type myosin; ▼, *mhc*$^-$ cells expressing E459V myosin; ◆, *mhc*$^-$ cells expressing E476K myosin; ▲, *mhc*A$^-$ cells expressing F481C/N483K myosin.

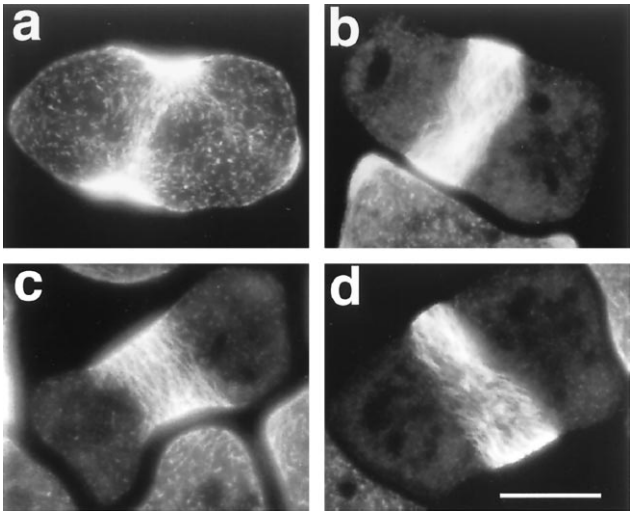

Figure 5. Localization of nonhydrolyzer myosins in the equatorial region. Cells were fixed and immunostained with anti-*Dictyostelium* myosin antibody. Cells expressing wild-type (a), E476K (b), E459V (c), and F481C/N483K mutant myosin (d) are shown. Bar, 10 μm.

Nonhydrolyzer Myosins Are Transported to the Equatorial Region with the Same Time Course as the Wild Type

The above observation that nonhydrolyzer myosins were concentrated in the equatorial region suggests that myosin is transported without its own ATPase and motor activities. However, it was also possible that the mutant myosins were transported very slowly to the equatorial region by using its very low residual ATPase activity. To distinguish between these two possibilities, we measured the rates of myosin transport to the equatorial region and also the rates of the residual ATPase activities.

For the real time tracing of myosin transport in vivo, we used the GFP-fusion technique developed by Moores *et al.* (1996). The E476K *mhc*A gene, fused to the GFP gene at the amino terminus (GFP-E476K), as well as the wild-type control (GFP-WT), were separately expressed in *mhc*A$^-$ cells. GFP-WT myosin normally accumulated in the equatorial region during mitosis (Figure 6). We observed that in some cells some GFP-WT myosin formed a single large aggregate beneath the cell membrane that did not move to the equatorial region. Even in this case, rest of the myosin normally accumulated in the equatorial region, and constriction of the contractile ring also proceeded normally. GFP-E476K myosin formed a similar aggregate in most of cells. Interestingly, many discrete filaments of myosin were readily observed in GFP-E476K cells, unlike GFP-WT. These filaments did not move noticeably in interphase cells but abruptly

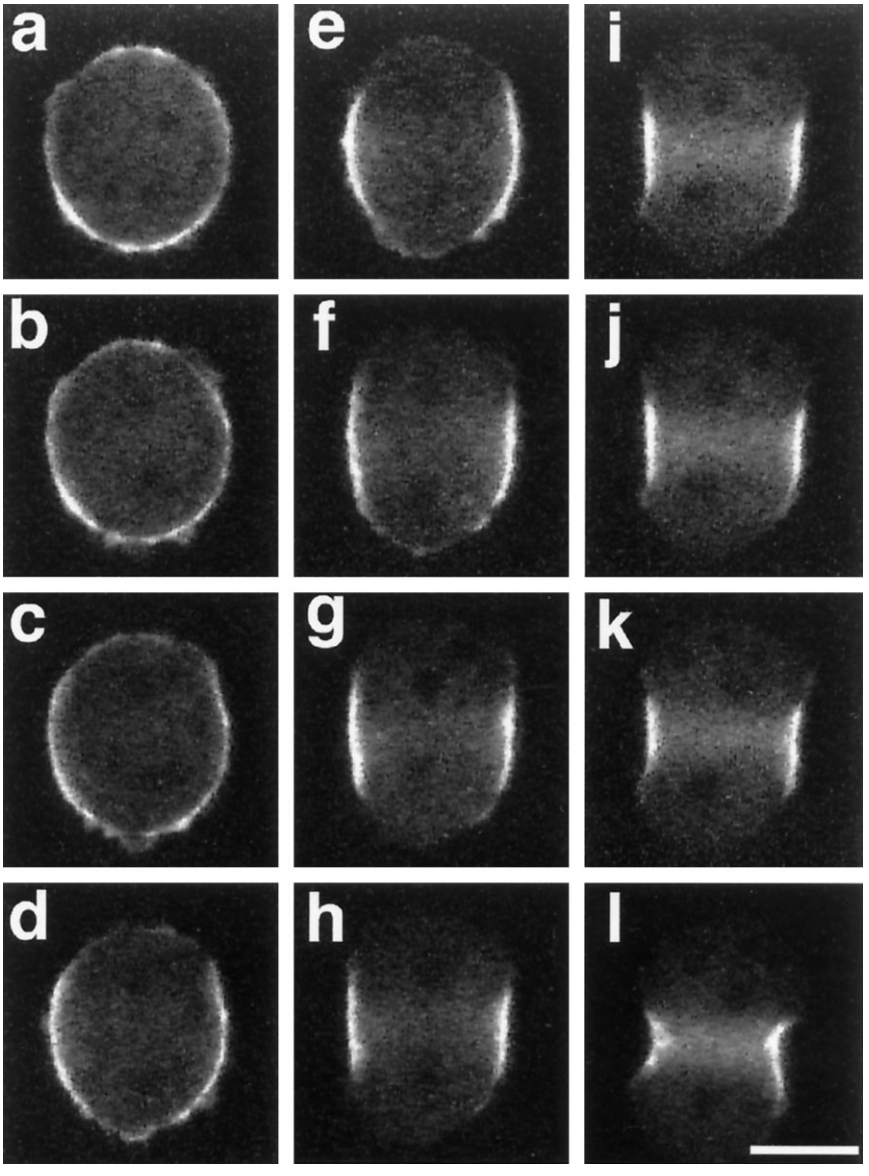

Figure 6. Accumulation of GFP-WT myosin in the equatorial region of a living cell. Fluorescence images were taken at 25-s intervals. Migration of myosin began at c and was completed at k. The contraction of the contractile ring commenced in l. Bar, 10 μm.

started to migrate toward the equatorial region in anaphase (Figure 7). At least under the present conditions of agar overlay, the furrow never constricted thereafter in GFP-E476K cells.

The time course of increase in the GFP fluorescence intensity in the equatorial region was compared between GFP-WT and GFP-E476K cells (Figure 8). The fold increase was slightly less in the case of GFP-E476K than GFP-WT possibly in part due to the aggregation of GFP-E476K myosin. Nonetheless, the time required to complete the accumulation of myosin in the equatorial region was not significantly different between GFP-E476K (t = 4.0 ± 0.6 min; n = 21) and GFP-WT (t = 3.9 ± 0.6 min; n = 14). These time courses were also comparable to that of IAF-labeled myosin in wild-type cells.

ATPase Activities of E476K

The steady-state ATPase activities of E476K myosin were undetectably too low and were not determined in the original study by Ruppel and Spudich (1996). We were able to detect its activities by preparing large quantities of the protein in a soluble form from overexpressing cell lines (M761–1R), and also by extending the reaction time to 1 h from the standard of 14–21 min.

The basal MgATPase activity of E476K/M761–1R was 0.0021 s^{-1}, which was 57-fold smaller than that of wild-type M761–1R (Table 1). The MgATPase activity of

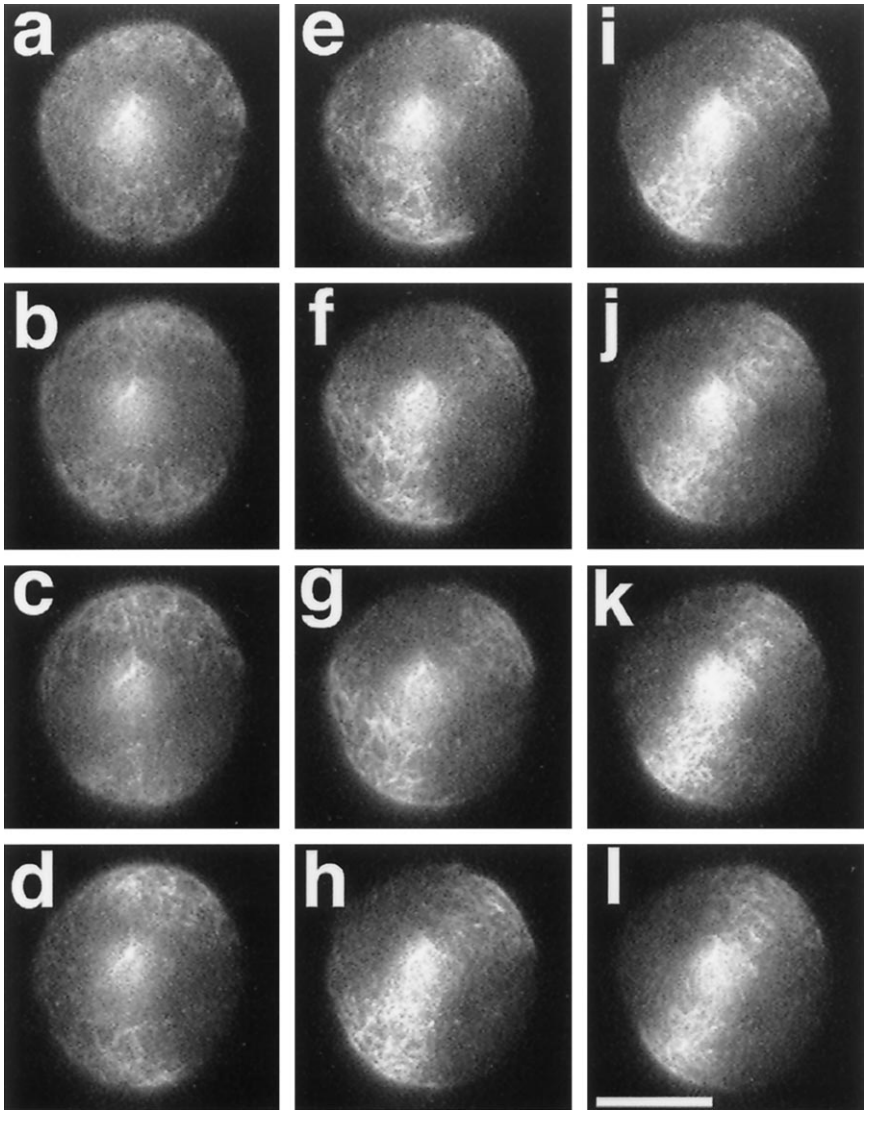

Figure 7. Accumulation of GFP-E476K myosin during mitosis of a living cell. Fluorescence images were taken at 0 s (a), 35 s (b), 1 min and 28 s (c), 2 min and 4 s (d), 2 min and 39 s (e), 3 min and 33 s (f), 4 min and 8 s (g), 4 min and 26 s (h), 5 min and 1 s (i), 5 min and 19 s (j), and 5 min and 37 s (k). Migration of myosin began at b and was completed at j. The contraction of this "pseudocontractile ring" did not occur. The round area of intense fluorescence shows the position of an out-of-focus intracellular aggregate of GFP-E476K myosin. Bar, 10 μm.

E476K/M761–1R was hardly activated by actin of up to 4 mg/ml, resulting in much larger difference in the actin-activated activities between the two proteins. The difference was 380-fold in the presence of 1 mg/ml actin and 580-fold when V_{max} values are compared.

The fold difference in the rate of accumulation of GFP myosin to the equatorial region and that of the actin-activated MgATPase activities are strikingly disproportionate, demonstrating that myosin can be transported toward the equatorial region and arranged to form the contractile ring structure without its own motor activities.

DISCUSSION

The equatorial stimulation model (Rappaport, 1991) and the polar relaxation model (White and Borisy, 1983; Bray and White, 1988), an extension of a theory originally proposed by Wolpert (1960), are the most recognized mechanisms of the cleavage furrow formation. The present study shows that the myosin increased uniformly in the cortical region, and then it moved to the equatorial region before the cleavage process started, which indicates that the stimulation of the myosin reorganization was not limited to the equatorial region. It is therefore difficult to explain the entire process of myosin reorganization by equatorial stimulation alone. The polar relaxation model hypothesizes that metaphase cells generate global and uniform cortical tension, and then an unknown stimulation from the mitotic spindle triggers relaxation of both polar cortex and the cortex to "contract" toward the equatorial region, depending on the active cortical

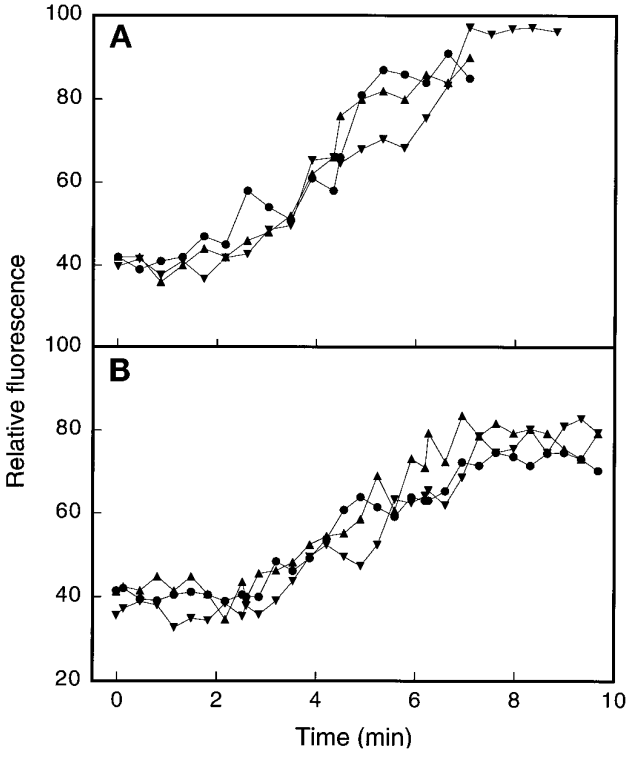

Figure 8. Increases of fluorescence intensity of GFP-WT (a) and GFP-E476K myosin (b) at the equatorial region during mitosis. The fluorescence intensity monitored at the center regions (10 × 10 pixels square) for three different cells are shown for each group (shown by different symbols).

tension (the cortical flow model; Bray and White, 1988). The cortical flow preceding cytokinesis is supported by many observations: the cortical transport of microinjected actin filaments toward the equator (Cao and Wang, 1990b) and the accumulation of surface receptors (Koppel *et al.*, 1982; Wang *et al.*, 1994) and particles attached to cell surface (Dan, 1954). Cortical tension is generated by active contraction of cortical actin and myosin filaments (Reines and Clarke, 1985; Yumura and Fukui, 1985; Pasternak *et al.*, 1989; Kuczmarski *et al.*, 1991; Yumura, 1991). Thus, implied in the cortical flow model is that the cortical flow is ultimately driven by the contractile activity of cortical actin and myosin (DeBiasio *et al.*, 1996).

We have tested this point by analyzing behavior of mutant myosins with no detectable contractile or motor activity. A number of such mutations are currently available in *Dictyostelium* and have been classified into several groups depending on the biochemical phenotype (Ruppel and Spudich, 1996). In this study we used the nonhydrolyzer class mutants. The primary defect in these mutant myosins is with the hydrolysis of ATP, and other steps in the ATPase cycle appear relatively normal (Ruppel and Spudich, 1996). In the presence of ATP, therefore, majority of the heads of such mutants carry bound ATP at the ATP binding site and are in the so called "weakly bound state" with actin. This constitutively weak affinity for actin is ideal in this study because it should allow weak association of myosin filaments with the cortical actin, without impeding possible cortical movement generated by other mechanisms.

Consistent with the nonfunctional phenotype in vitro, all three nonhydrolyzer mutant myosins were unable to complement the defects of myosin null cells, such as the inability to divide in suspension culture and form fruiting bodies (Ruppel and Spudich, 1996; Figure 4). Surprisingly, however, our immunofluorescence observation demonstrated that all three mutant were correctly transported to the equatorial region of telophase cells (Figure 5). Furthermore, the mutant myosin filaments were aligned parallel to the equator. The fact that both wild-type and E476K myosins were accumulated in the equatorial region at similar rates, despite the large difference in the actin-activated MgATPase activities, lead us to conclude that the motor activity of myosin is not required for the transport of myosin to the equatorial region. We also concluded that the E476K myosin, and probably wild-type myosin as well, is passively carried to the equatorial region by some other mechanism. We often observed that E476K filaments moved some distance toward the equator without being disassembled (our unpublished observations). A similar observation has been reported for the movement of myosin filaments in di-

Table 1. ATPase activities of M761-1R and E476K/M761-1R myosin head fragments

	Basal MgATPase (s^{-1})	Actin-activated MgATPase (s^{-1})		High salt CaATPase (s^{-1})
		Actin	V_{max}	
M761-1R	0.12	0.94	1.5	1.5
E476K/M761-1R	0.0021 ± 0.0002	0.0025 ± 0.0005	0.0026	0.0021

Some assays were repeated three times from two independent preparations, and the data are the mean ±SD. Actin was added at 1 mg/ml.

viding fibroblasts (DeBiasio *et al.*, 1996). Thus, the transport of myosin filaments appears to be mediated by association with the cortical components rather than de novo localized assembly of myosin filaments in the equatorial region and disassembly in the polar region. This hypothesis is supported by our recent finding that another mutant myosin, which is severely impaired in the ability to disassemble to monomers, is equally well concentrated in the equatorial region (Yumura and Uyeda, 1997).

The passive transport of myosin filaments is reminiscent of the flow of actin filaments toward the equatorial region (Cao and Wang, 1990a). Thus, the available evidence suggests that such cortical flow of actin filaments is also independent of myosin's motor activity or cortical tension. This speculation is consistent with the observations of Yumura and Uyeda (1997) and Neujahr *et al.* (1997) that actin filaments accumulate in the equatorial region even in cells devoid of myosin filaments.

Relevant to the cortical equatorial movement of actin and myosin filaments, Jay and Elson (1992) have shown that surface particles are carried to the posterior of polarized *Dictyostelium mhc*A$^-$ cells. Since the contractile ring is transformed to the posterior region of daughter cells after the cleavage is complete, it seems reasonable to assume that there is a common underlying motile mechanism between the movement of cortical actin and myosin filaments toward the equatorial region and the movement of surface particles toward the posterior of interphase cells. Interestingly, our estimate of the average velocity of myosin filaments toward the equatorial region (2.9 μm/min) is comparable to that of beads on *mhc*A$^-$ cells (2.59 μm/min; Jay and Elson, 1992). These velocities are also comparable to that of the transport of particles on the surface and injected actin filaments toward the equatorial region in dividing animal cells (Cao and Wang, 1990b; Hird and White, 1993; Wang *et al.*, 1994). It would be tempting to assume that other "unconventional" myosins are involved in powering this process. Consistent with this model, concentration of myosin I in the midbody region has been reported in mammalian cells (Brecker and Burnside, 1994). Immunofluorescence staining has shown that myosin IB is primarily localized to the polar region of dividing *Dictyostelium* cells (Fukui *et al.*, 1989). However, *Dictyostelium* has been shown by low-stringency hybridization to carry 13 putative unconventional myosin loci, including six myosin I genes (Uyeda and Titus, 1997), and localization of these gene products to the equatorial region is yet to be examined. Alternatively, dynamic structural changes of the actin cytoskeleton may be driving the active cortical flow. In either case, we speculate that myosin II is transported passively by associating with the cortical actin cytoskeleton.

Movement of myosin filaments to the equatorial region can be explained by other models that do not require active cortical flow. For instance, it has been hypothesized that phosphorylation of regulatory light chain or heavy chain of myosin determines the myosin localization (Kolega and Taylor, 1980; Spudich, 1989; Yumura and Kitanishi-Yumura, 1992, 1993; Egelhoff *et al.*, 1993). However, mutant myosins that cannot be phosphorylated on the heavy chain (Egelhoff *et al.*, 1991a, 1993) or on the regulatory light chain (Uyeda and Spudich, 1993; Ostrow *et al.*, 1994) are at least partially functional in vivo. Our recent immunofluorescence studies further demonstrated that these mutant myosins are properly localized to the contractile ring, unambiguously eliminating the essential roles of phosphorylation regulation of myosin in its localization to the contractile ring (Yumura and Uyeda, 1997).

Another still plausible model assumes that an unidentified protein with a strong affinity for myosin is specifically localized in the equatorial region of a dividing cell, and myosin is attracted to these regions in a passive manner. This model is supported by a cytological study of Schroeder and Otto (1988), who observed that myosin is still bound specifically to actin-free contractile rings. This possibility is further supported by segregation of muscle and nonmuscle myosins coexpressed in nonmuscle cells. Skeletal muscle myosin filaments were present in the cytoplasm and were not incorporated into stress fibers, whereas nonmuscle myosin filaments were (Moncman *et al.*, 1993).

In summary, we have demonstrated that the contractile activity of myosin is not required for the transport of myosin filaments to the equatorial region of dividing *Dictyostelium* cells. This does not necessarily rule out the possible involvement of active cortical flow, powered by unconventional myosins, or structural changes of the actin cytoskeleton. Further experiments are warranted to test this and other hypotheses.

ACKNOWLEDGMENTS

We thank Dr. Kathleen Ruppel for the gift of the nonhydrolyzer mutant myosin genes, Sheri Moores for the gift of the GFP-myosin expression plasmid, and Dr. James Spudich for allowing us to use these materials before publication. Dr. Dietmar Manstein also kindly provided us with the M761–1R construct before publication. We also thank Dr. Roger Tsien for the kind gift of the *S65T GFP* gene. This work is partly supported by a Grant-in-Aid for Scientific Research from the Ministry of Education Science and Culture of Japan to S.Y.

REFERENCES

Anson, M., Geeves, M.A., Kurzawa, S.E., and Manstein, D.J. (1996). Myosin motors with artificial lever arms. EMBO J. *15*, 6069–6074.

Ausubel, F., Brent, R., Kingston, R.E., Moore, D.D., Seidman, J.G., Smith, J.A., and Struhl, K. (1994). Current Protocols in Molecular Biology, New York: John Wiley & Sons.

Bray, D., and White, J.G. (1988). Cortical flow in animal cells. Science *239*, 883–888.

Brecker, J., and Burnside, B. (1994). Myosin I localizes to the midbody region during mammalian cytokinesis. Cell Motil. Cytoskeleton *29*, 312–320.

Cao, L.-G., and Wang, Y.-L. (1990a). Mechanism of the formation of contractile ring in dividing cultured animal cells. I. Recruitment of preexsiting actin filaments into the cleavage furrow. J. Cell Biol. *110*, 1089–1095.

Cao, L.-G., and Wang, Y.-L. (1990b). Mechanism of the formation of contractile ring in dividing cultured animal cells. II. Cortical movement of microinjected actin filaments. J. Cell Biol. *111*, 1905–1911.

Chu, Q., and Fukui, Y. (1996). In vivo dynamics of myosin II in *Dictyostelium* by fluorescent analogue cytochemistry. Cell Motil. Cytoskeleton *35*, 254–268.

Dan, K. (1954). The cortical movement in *Arbacia punctulata* eggs through cleavage cycle. Embryologia *2*, 111–122.

DeBiasio, R.L., LaRocca, G.M., Post, P.L., and Taylor, D.L. (1996). Myosin II transport, organization, and phosphorylation: evidence for cortical flow/isolation-contraction coupling during cytokinesis and cell locomotion. Mol. Biol. Cell *8*, 1259–1282.

De Lozanne, A., and Spudich, J.A. (1987). Disruption of the *Dictyostelium* myosin heavy chain gene by homologous recombination. Science *236*, 1086–1091.

Egelhoff, T.T., Brown, S.S., and Spudich, J.A. (1991a). Spatial and temporal control of nonmuscle myosin localization: identification of a domain that is necessary for myosin filament disassembly in vivo. J. Cell Biol. *112*, 677–688.

Egelhoff, T.T., Lee R.J., and Spudich J.A. (1993). *Dictyostelium* myosin heavy chain phosphorylation sites regulate myosin filament assembly and localization in vivo. Cell *75*, 363–371.

Egelhoff, T.T., Titus, M.A., Manstein, D.J., Ruppel, K.M., and Spudich, J.A. (1991b). Molecular genetic tools for study of the cytoskeleton in *Dictyostelium*. Methods Enzymol. *196*, 319–334.

Fukui, Y., Lynch, T.J., Brzeska, H., and Korn, E.D. (1989). Myosin I is localized at the leading edges of locomoting *Dictyostelium* amoebae. Nature *341*, 328–331.

Gordon, D.J., Yang, Y.Z., and Korn, E.D. (1976). Polymerization of *Acanthamoeba* actin. Kinetics, thermodynamics, and co-polymerization with muscle actin. J. Biol. Chem. *251*, 7474–7479.

Heim, R., Cubitt, A., B., and Tsien, R.Y. (1995). Improved green fluorescence. Nature *373*, 663–664.

Hird, S.N., and White, J.G. (1993). Cortical and cytoplasmic flow polarity in early embryonic cells of *Caenorhabditis elegans*. J. Cell Biol. *121*, 1343–1355.

Jay, P.T., and Elson, E.L. (1992). Surface particle transport mechanism independent of myosin II in *Dictyostelium*. Nature *356*, 438–440.

Kitanishi-Yumura, T., and Fukui, Y. (1989). Actomyosin organization during cytokinesis: reversible translocation and differential redistribution in *Dictyostelium*. Cell Motil. Cytoskeleton *12*, 78–89.

Knecht, D.A., and Loomis, W.F. (1987). Antisense RNA inactivation of myosin heavy chain gene expression in *Dictyostelium discoideum*. Science *236*, 1081–1086.

Kodama, T., Fukui, K., and Kometani, K. (1986). The initial phosphate burst in ATP hydrolysis by myosin and subfragment-1 as studied by a modified malachite green method for determination of inorganic phosphate. J. Biochem. *99*, 1465–1472.

Kolega, J., and Taylor, D.L. (1993). Gradients in the concentration and assembly of myosin II in living fibroblasts during locomotion and fiber transport. Mol. Biol. Cell *4*, 819–836.

Koppel, D.E., Oliver, J.M., and Berlin, R.D. (1982). Surface functions during mitosis. III. Quantitative analysis of ligand-receptor movement into the cleavage furrow: diffusion vs. flow. J. Cell Biol. *93*, 950–960.

Kuczmarski, E.R., Palivos, L., Aguado, C., and Yao, Z.L. (1991). Stopped-flow measurement of cytoskeletal contraction: *Dictyostelium* myosin II is specifically required for contraction of amoeba cytoskeletons. J. Cell Biol. *114*, 1191–9.

Mabuchi, I. (1986). Biochemical aspects of cytokinesis. Int. Rev. Cytol. *101*, 175–213.

Mabuchi, I., and Okuno, M. (1977). The effect of myosin antibody on the division of starfish blastomeres. J. Cell Biol. *74*, 251–263.

Manstein, D.J., and Hunt, D.M. (1995). Overexpression of myosin motor domains in *Dictyostelium*: screening of transformants and purification of the affinity tagged protein. J. Muscle Res. Cell Motil. *16*, 325–332.

Moncman, C.L., Rindt, H., Robbins, J., and Winkelmann, D.A. (1993). Segregated assembly of muscle myosin expressed in nonmuscle cells. Mol. Biol. Cell *4*, 1051–1067.

Moores, S., Sabry, J.H., and Spudich, J.A. (1996). Myosin dynamics in live *Dictyostelium* cells. Proc. Natl. Acad. Sci. USA *93*, 443–446.

Neujahr, R., Heizer, C., and Gerisch, G. (1997). Myosin II-independent processes in mitotic cells of *Dictyostelium discoideum*: redistribution of the nuclei, rearrangements of the actin system, and formation of the cleavage furrow. J. Cell Sci. *110*, 123–137.

Ostrow, B.D., Chen, P., and Chisholm, R.L. (1994). Expression of a myosin regulatory light chain phosphorylation site mutants complements the cytokinesis and developmental defects of *Dictyostelium* RMLC null cells. J. Cell Biol. *127*, 1945–1955.

Pasternak, C., Spudich, J.A., and Elson, E.L. (1989). Capping of surface receptors and concomitant cortical tension are generated by conventional myosin. Nature *341*, 549–551.

Rappaport, R. (1991). Cytokinesis. In: Oogenesis, Spermatogenesis and Reproduction, ed. K.H. Kinne, Basel, Switzerland: Karger, 1–36.

Reines, D., and Clarke, M. (1985). Immunochemical analysis of the supramolecular structure of myosin in contractile cytoskeletons of *Dictyostelium* ameobae. J. Biol. Chem. *260*, 14248–14254.

Ruppel, K.M., and Spudich, J.A. (1995). Myosin motor function: structural and mutagenic approaches. Curr. Opin. Cell Biol. *7*, 89–93.

Ruppel, K.M., and Spudich, J.A. (1996). Structure-function studies of the myosin motor domain: importance of the 50-kDa cleft. Mol. Biol. Cell *7*, 1123–1136.

Ruppel, K.M., Uyeda, T.Q.P., and Spudich, J.A. (1994). Role of highly conserved lysine 130 of myosin motor domain. J. Biol. Chem. *269*, 18773–18780.

Schroeder, T.E., and Otto, J.J. (1988). Immunofluorescent analysis of actin and myosin in isolated contractile rings of sea urchin eggs. Zool. Sci. *5*, 713–725.

Spudich, J.A. (1989). In pursuit of myosin function. Cell Regul. *1*, 1–11.

Spudich, J.A., and Watt, A. (1971). The regulation of rabbit skeletal muscle contraction. J. Biol. Chem. *246*, 6013–6020.

Strome, S. (1993). Determination of cleavage planes. Cell *72*, 3–6.

Sussman, S. (1987). Cultivation and synchronous morphogenesis of *Dictyostelium* under controlled experimental conditions. Methods Cell Biol. *28*, 9–29.

Uyeda, T.Q.P., and Spudich, J.A. (1993).A functional recombinant myosin II lacking a regulatory light chain-binding site. Science *262*, 1867–1870.

Uyeda, T.Q.P., and Titus, M.A. (1997). The Myosins of *Dictyostelium*. Dictyostelium—The Model Organism for Basic Biology, Tokyo: Universal Academy Press.

Wang, Y.-L., Silverman, J.D., and Cao, L.-G. (1994). Single particle tracking of surface receptor movement during cell division. J. Cell Biol. *127*, 963–971.

White, J.G., and Borisy, G.G. (1983). On the mechanism of cytokinesis in animal cells. J. Theor. Biol. *101*, 289–316.

Wolpert, L. (1960). The mechanics and mechanism of cleavage. Int. Rev. Cytol. *10*, 163–216.

Yumura, S. (1991). Contraction of *Dictyostelium* ghosts reconstituted with myosin II. Cell Struct. Funct. *16*, 481–488.

Yumura, S. (1996). Rapid redistribution of myosin II in living *Dictyostelium* amoebae, as revealed by fluorescent probes introduced by electroporation. Protoplasma *192*, 217–227.

Yumura, S., and Fukui, Y. (1985). Reversible cyclic AMP-dependent change in distribution of myosin thick filaments in *Dictyostelium*. Nature *314*, 194–196.

Yumura, S., and Kitanishi-Yumura, T. (1992). Release of myosin II from the membrane-cytoskeleton of *Dictyostelium discoideum* mediated by heavy-chain phosphorylation at the foci within the cortical actin network. J. Cell Biol. *117*, 1231–1239.

Yumura, S., and Kitanishi-Yumura, T. (1993). A mechanism for the intracellular localization of myosin filaments in the *Dictyostelium* amoebae. J. Cell Sci. *105*, 233–242.

Yumura, S., Matsuzaki, R., and Kitanishi-Yumura, T. (1995). Introduction of macromolecules into living *Dictyostelium* cells by electroporation. Cell Struct. Funct. *20*, 185–190.

Yumura, S., Mori, S., and Fukui, Y. (1984). Localization of actin and myosin for the study of amoeboid movement in *Dictyostelium* using improved immunofluorescence. J. Cell Biol. *99*, 894–899.

Yumura, S., and Uyeda, T.Q.P. (1997). Myosin II can be localized to the cleavage furrow and to the posterior region of *Dictyostelium* amoebae without control by phosphorylation of myosin heavy chain and light chains. Cell Motil. Cytoskeleton *36*, 313–322.